Acta Crystallographica Section B
Structural Science
ISSN 0108-7681

Description of $Ba_{1+x}Ni_xRh_{1-x}O_3$ with x = 0.1170 (5) in superspace: modulated composite *versus* modulated-layer structure

Andreas Schönleber,[a]*‡ F. Javier Zúñiga,[a] J. Manuel Perez-Mato,[a] Jacques Darriet[b] and Hans-Conrad zur Loye[c]

[a]Departamento de Física de la Materia Condensada, Facultad de Ciencia y Tecnología, Universidad del País Vasco, Apartado 644, 48080 Bilbao, Spain, [b]Institut de Chimie de la Matière Condensée de Bordeaux, 87 Avenue du Dr A. Schweizer, 33608 Pessac CEDEX, France, and [c]Department of Chemistry and Biochemistry, University of South Carolina, Columbia, SC 29208, USA

‡ Present address: Lehrstuhl für Kristallographie, Universität Bayreuth, BGI Gebäude, 95440 Bayreuth, Germany.

Correspondence e-mail: andreas.schoenleber@uni-bayreuth.de

Received 8 September 2005
Accepted 25 November 2005

The structure of the compound $Ba_{1+x}Ni_xRh_{1-x}O3$ [x = 0.1170 (5)] has been analyzed at room temperature within the (3 + 1)-dimensional superspace approach using single-crystal X-ray diffraction data. Two different models are presented, the compound is refined as modulated composite as well as modulated-layer structure. In both models discontinuous atomic domains are applied to describe the structural modulations. While the first approach stresses the pseudo-one-dimensional constitution, the latter highlights the layered character of these structures.

1. Introduction

$Ba_{1+x}Ni_xRh_{1-x}O_3$ with x = 0.1170 (5) is a member of the family of trigonal compounds $A_{1+x}A'_xB_{1-x}O_3$ with $x \in [0,\frac{1}{2}]$. In general, A is an alkaline earth element, A' represents a divalent and B a tetravalent cation. These structures are closely related to the 2H hexagonal perovskite and are built up in a first approximation by a hexagonal close packing of $[A_3O_9]$ and $[A_3A'O_6]$ layers. Applying the relation $x = n/(3m + 2n)$, the formula can be written as $A_{3m+3n}A'_nB_{3m+n}O_{9m+6n}$ with the integers m and n being the numbers of layers of $[A_3O_9]$ and $[A_3A'O_6]$, respectively (Perez-Mato *et al.*, 1999). This mixed hexagonal-like stacking creates two types of interstices: octahedra as coordination polyhedra for the B cations and trigonal prisms for the A' cations (Darriet & Subramanian, 1995; Blake *et al.*, 1998; Perez-Mato *et al.*, 1999). The lattice parameter a of these structures corresponds with $a \simeq 10$ Å to $(3^{1/2})a_{per}$, while the c parameter depends on the actual values of m and n and can be rather large (with a_{per} being the lattice parameter of the perovskite structure).

Being either incommensurately modulated or long-period structures, it is usually convenient to use the superspace formalism (de Wolff, 1974; Janner & Janssen, 1980*a*,*b*; Janssen *et al.*, 1992; van Smaalen, 1995) for a quantitative analysis of these compounds. The structures of several materials belonging to this family have already been published, showing the efficiency of the superspace approach while dealing with such series of composition-flexible materials. These structures have been described mainly as modulated composites (Ukei *et al.*, 1993; Battle *et al.*, 1997, 1998; Evain *et al.*, 1998; Gourdon *et al.*, 1999; Perez-Mato *et al.*, 1999; Zakhour-Nakhl, Claridge *et al.*, 2000; Zahhour-Nakhl, Darriet *et al.*, 2000; Zakhour-Nakhl, Weill *et al.*, 2000; El Abed *et al.*, 2001). However, in a more recent publication by Elcoro *et al.* (2003) an alternative superspace model is presented in which the structural description in terms of layers is kept and the structures are understood as modulated-layer structures.

For the present work, the target of crystal growing was the compound $Ba_{1+x}Ni_xRh_{1-x}O_3$ with the stoichiometric para-

Table 1
Crystal data for the different cell settings.

The index '*C*' of the modulation wavevector component refers to the *modulated composite* with subsystem 1 and the index '*L*' to the *modulated-layer structure* with subsystem 2 as reference. The centring *X* in the superspace group of cell setting 2 is explained in the text.

	Physical space supercell	Superspace cell setting 1	Superspace cell setting 2
Chemical formula	$Ba_{10}NiRh_8O_{27}$	$Ba_{1+x}Ni_xRh_{1-x}O$	$BaNi_yRh_{1-2y}O_{3(1-y)}$
Stoichiometric parameter	–	$x = 0.1170$ (5)	$y = x/(1+x) = 0.1047$ (7)
Formula weight	2687.31	299.14	267.81
$F(000)$	–	389	696
Z	3	3	6
a (Å)	10.0576 (8)	10.0576 (8)	10.0576 (5)
c (Å)	23.205 (3)	2.5862 (8)	4.6306 (7)
V (Å^3)	2032.8 (3)	226.6 (5)	405.7 (7)
q	–	$\gamma_C = 0.5585$ (5)	$\gamma_L = 0.2095$ (7)
D_x (Mg m^{-3})	6.5803	6.5754	6.5754
Symmetry	$P321$	$R\bar{3}m(00\gamma)0s$	$X\bar{3}c1(00\gamma)000$

Table 2
Experimental data.

	Three-dimensional supercell
Temperature (K)	293
Crystal form	Hexagonal prismatic
Crystal size (mm^3)	0.05 × 0.06 × 0.08
Colour	Metallic black
Number of measured and observed reflections	46 025/8677
Number of unique reflections	8239/2088
Absorption correction	Gaussian integration
μ (mm^{-1})	19.747
R_{int}	5.85/5.15
Coverage	96.78% at $\theta = 40.21°$

meter $x = 1/9$. An analysis of the single-crystal X-ray diffraction data made it clear that the stoichiometry is better described by $x = 0.1170$ (5) $\simeq 2/17 \simeq 5/43$. In this contribution the results of the superspace refinement for both descriptions, *i.e.* modulated composite and modulated-layer structure, are presented. In both models discontinuous atomic domains in superspace (crenel and/or sawtooth functions) are introduced and constitute a fundamental part of the structural modulation.

2. Experimental

For sample preparation standard methods of solid-state chemistry were applied, *i.e.* the crystals were grown by K_2CO_3 flux synthesis. Details are described in Henley *et al.* (1999).

The data collection was carried out on an Oxford Diffraction Xcalibur diffractometer with CCD detector. A single crystal with the shape of a hexagonal prism was carefully chosen. The data set was consistent with a primitive Bravais hexagonal lattice and could be approximately described in a first attempt by a supercell lattice with $a \simeq 10.06$ and $c \simeq 23.22$ Å, $V \simeq 2036.6$ Å^3. A thorough inspection of the diffraction pattern presented the misfit character of the structure by exhibiting two distinct main periodicities along **c***, and additionally some satellite reflections. The intensities of the first subsystem (with periodicity c_1^*) seemed somewhat weaker than those of the second subsystem (periodicity c_2^*), which is consistent with the atomic numbers of the constituting atoms.

With a *hklm* integer indexing in (3 + 1)-dimensional superspace, the cell and modulation wavevector parameters were refined with the program *NADA* (Schönleber *et al.*, 2001). Both subsystems were applied in succession as the reference system, the two distinct lattice parameters c_1 and c_2 could be defined as c_1 being close to $\frac{1}{2}c_{per}$ and c_2 corresponding to c_{per} (Table 1). The relation between the modulation wavevector component and the c parameter is $\gamma_c = c_1/c_2$ and $\gamma'_L = (c_2/c_1) = 1/\gamma_C$ (the index '*C*' refers to the *modulated composite* with subsystem 1 and the index '*L*' to the *modulated-layer structure* with subsystem 2 as a reference). To keep these parameters in the usual range [0, 1], the new parameter $\gamma_L = N \pm \gamma'_L$ was introduced, in the present case with $\gamma_L = 2 - \gamma'_L$.

Integration of intensities and data reduction were carried out with the *CrysAlis* Software Package (Oxford Diffraction, 2003) in three-dimensional space with the 10 × 10 × 23 Å^3 supercell approximation and *hkl* indexing. A successive absorption correction (Gaussian integration method) was carried out with *JANA*2000 (Petricek *et al.*, 2000) in this supercell setting. The *hkl* data were then transformed with *JANA*2000 (Petricek *et al.*, 2000) into the respective *hklm* indexing for the *modulated composite* and for the *modulated-layer structure*. Applying the two different reference systems and modulation-wavevector parameter resulted in a different indexing of the diffraction pattern with different sets of main and satellite reflections. Details on data reduction in the different cell settings are given in Tables 1 and 2.

During data reduction and refinement the crystal was supposed to be pseudo-merohedrally twinned with perfect superposition of the two lattices (which is quite common in those materials). The matrix between the two twin domains can be expressed as ($\bar{1}$ 0 0/0 $\bar{1}$ 0/0 0 1). The refined twin volume ratios are approximately 2/3:1/3.

3. Superspace models

The two different models *modulated composite* (the general model was proposed by Perez-Mato *et al.*, 1999) and *modulated-layer structure* (the general model was developed by Elcoro *et al.*, 2003) were applied during structure refinement. In both approaches discontinuous atomic domains in superspace, *i.e.* crenel functions (Petříček *et al.*, 1995) and sawtooth functions (Petricek *et al.*, 1990) were implemented in the models, as they constitute the fundamental part of the description of the structural modulation.

3.1. Stoichiometry

The relation between stoichiometric composition and modulation wavevector parameter is given as

$(c_2/2)/c_1 = 1/(1+x)$ (Evain *et al.*, 1998; Perez-Mato *et al.*, 1999). With the refined lattice parameters (Table 1) x_{calc} = 0.1170 (5). This can be approximated by the two commensurate values x = 2/17 and x = 5/43. The modulation vector components can be expressed as γ_C = 19/34 and γ_L = 4/19 for the first and γ_C = 24/43 and γ_L = 5/24 for the latter. All these theoretical values describe the refined ones within 2σ. The chemical formula of the present compound is then written for x = 2/17 as $Ba_{10.059}Ni_{1.059}Rh_{7.941}O_{27}$ with lattice parameter $c_S = 34c_1 = 19c_2 \simeq 87.9$ Å and for x = 5/43 as $Ba_{10.047}Ni_{1.047}Rh_{7.953}O_{27}$ with $c_S = 43c_1 = 24c_2 \simeq 111.2$ Å.

Consequently, the structures could be described within experimental accuracy as commensurately modulated. However, as the denominator in γ is quite large, the commensurate structure becomes incommensurate in a practical sense and the distinction between the two cases is not essential for a precise structural analysis (Perez-Mato *et al.*, 1987, 1999). Hence, structure refinement was performed in (3 + 1)-dimensional superspace applying the incommensurate option.

3.2. Modulated composite

The starting model for refinement was proposed by Perez-Mato *et al.* (1999). All structural parameters are given in the supplementary material[1] as a function of the stoichiometric parameter x. The *modulated composite* consists of two subsystems with subsystem 1 being formed by the $(A',B)O_3$ columns and subsystem 2 by the A cations. It is common to use the columns of subsystem 1 as a reference system. The superspace group was chosen to be $R\bar{3}m(000\gamma)0s$, which is compatible with the observed reflection conditions $hklm$: $h - k - l = 3n$ and $hhlm$: $m = 2n$.

As a result of the hexagonal close-packing arrangement of the layers (Elcoro *et al.*, 2003), the sequences of octahedra and prisms, which can be unequivocally deduced from the stoichiometry through a Farey tree (Neville, 1950), as explained in Perez-Mato *et al.* (1999), is for the case x = 2/17 = (1 + 1)/(9 + 8): [8Oct–1Pr–7Oct–1Pr] and for the case x = 5/43 = (1 + 1 + 1 + 1 + 1)/(9 + 9 + 8 + 9 + 8): [8Oct–1Pr–8Oct–1Pr–7Oct–1Pr–8Oct–1Pr–7Oct–1Pr].

An idealized arrangement of the structure for the case x = 2/17 is shown in Fig. 1. There are three columns and chains per asymmetric unit with a small offset between neighbouring ones. Each column contains the same sequence of octahedra and prisms. In the incommensurate model the [8Oct–1Pr–7Oct–1Pr] periodic succession of the sequential units is disturbed by an aperiodic insertion of [8Oct–1Pr–8Oct–1Pr–7Oct–1Pr], because the observed γ component is slightly smaller than the rational fraction 19/34, implying a octahedra-to-prism site ratio, which is with *ca* 15.1:2 slightly larger than the commensurate 15:2 (Evain *et al.*, 1998). For the case where x = 5/43 it is slightly smaller.

[1] Supplementary data for this paper are available from the IUCr electronic archives (Reference: CK5013). Services for accessing these data are described at the back of the journal.

Following Perez-Mato *et al.* (1999), the atoms of subsystem 1 (Ni, Rh and O) were described by sawtooth functions. For

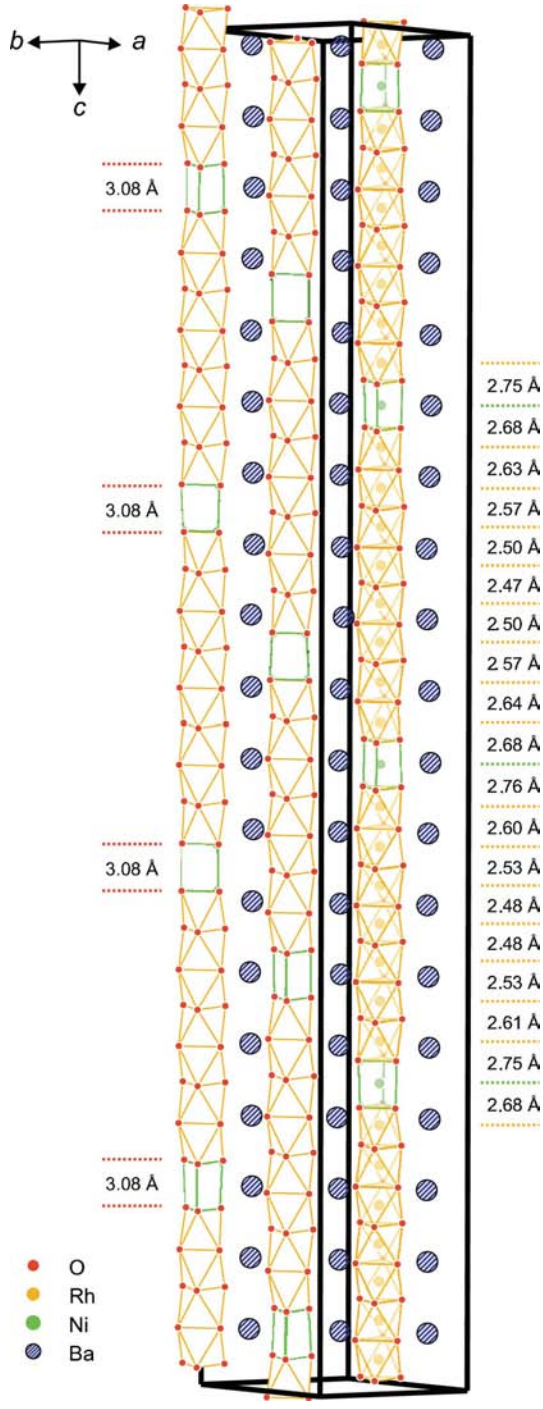

Figure 1
Idealized arrangement of columns and chains for a compound with the stoichiometry x = 2/17. The modulation wavevector component is γ_C = 19/34, the ratio between octahedra and prisms is 15:2. For the sake of better presentation, the polyhedra of the right column are drawn in a transparent mode, the other two are solid. On the right side, interatomic distances for the central atoms of the polyhedra, *i.e.* Rh—Ni and Rh—Rh, respectively, are indicated, as well as O—O distances on the left side for the height of the trigonal prisms (these values are derived from this idealized arrangement).

Table 3
Refinement data.

The different number of all reflections in the two models is due to the fact that for the *modulated composite* the satellite reflections of third and fourth order were discarded during refinement.

	Modulated composite	*Modulated-layer structure*
Refinement on	*F*	*F*
S	1.26	1.31
Reflections (all)	1127	1195
Main/first order/second order	415/529/183	254/657/284
Parameters	53	53
Twin volume fractions	0.6787 (16), 0.3213 (16)	0.6787 (17), 0.3213 (17)
R_{obs}/wR_{obs} (all)	0.0379/0.0481	0.0382/0.0504
R_{obs}/wR_{obs} (main reflections)	0.0314/0.0396	0.0274/0.0341
R_{obs}/wR_{obs} (first-order satellites)	0.0442/0.0498	0.0415/0.0522
R_{obs}/wR_{obs} (second-order satellites)	0.0662/0.0857	0.0605/0.0710
Weighting scheme	$[\sigma^2(F) + (0.025F)^2]^{-1}$	$[\sigma^2(F) + (0.025F)^2]^{-1}$
$(\Delta/\sigma)_{max}$	−0.0002	0.0002
$\Delta\rho_{max}$, $\Delta\rho_{min}$ (e Å^{-3})	1.94/−2.41	1.75/−2.35

those of subsystem 2 (Ba1 and Ba2), also in a first approach, sawtooth functions were applied. However, in further steps of refinement, the modulations (amplitudes of the sawtooth functions) appeared to be very small. Therefore, it seemed more appropriate to model them by crenel functions. The refinement of the structure in (3 + 1)-dimensional superspace was performed with the program *JANA*2000 (Petricek *et al.*, 2000) in cell setting 1. In addition to the main reflections, satellite reflections up to second order were used during refinement based on their intensities [$I_{obs} \geq 3\sigma(I_{obs})$]. The final residual values for the refining 53 parameters were R_{obs} = 0.0379 and wR_{obs} = 0.0481 for the observed reflections. More details on the refinement are given in Table 3.

In the first step of refinement, the displacive modulation of the atoms was described only by sawtooth functions for the Ni, Rh and O atoms and crenel functions for the Ba1 and Ba2 atoms, as defined by Perez-Mato *et al.* (1999). In this ideal model, the widths and centres of the crenel/sawtooth functions are fully determined by symmetry and geometrical considerations and do not need to be refined, *i.e.* the widths Δ are determined by stoichiometry and the centres x_4 are at special positions. The amplitudes δ of the sawtooth functions were refined applying the relations between the Ni, Rh and O atoms, as given in the supplementary material (assuming parallel sawtooths). In a second step, the amplitude δ of the sawtooth for Ni atoms was fixed and those for Rh and O were refined without any restriction. As a result, the sawtooths of the three atoms were no longer perfectly parallel. In a next step, all amplitudes δ of the sawtooth functions were fixed to their refined values, and for Rh and O the sawtooth functions and for Ba2 the crenel function were combined (superposed) with harmonic displacive modulation functions. To do so, orthogonalization procedures were introduced to reduce the correlations. Since the widths of the crenel/sawtooth functions are smaller than 1, the atomic modulation functions are no longer defined for all values along x_4 and thus the orthogonality condition is not fulfilled for the set of harmonic functions (Petříček *et al.*, 1995). Therefore, this orthogonalization is necessary. In the final model, the Rh and O atoms were refined with a sawtooth function, and two additional waves for the displacive modulation and two waves for the modulation of the anisotropic ADPs (atomic displacement parameters), the Ba2 atom with a crenel function and one additional wave for the displacive modulation. The modulations of the Ni and Ba1 atoms are described only with the sawtooth function and crenel function, respectively. The Fourier maps with the atomic domains are given in Figs. 2–4.

This structure modeling with orthogonalized functions improved the original description with pure crenel and sawtooth functions significantly. However, the refinement converged only while a damping factor of 0.35 or smaller was applied. The ADP tensor of the Ni atom was not positive definite and a new difference Fourier synthesis series revealed important positive residues around and negative residues on the Ni position (Fig. 5). For the compound $Sr_{1.2872}NiO_3$, Evain *et al.* (1998) described the position of the Ni atoms in the trigonal prisms as split over five positions. In the present case splitting of the position was not successful, every attempt resulted in a divergent refinement and/or negative ADPs for the Ni atoms. Therefore, a nonharmonic behaviour of the ADPs was considered and Gram–Charlier fourth-order tensor coefficients were introduced into the refinement (Kuhs, 1992; Evain *et al.*, 1998). With this five additional parameters, not only could positive ADPs for the Ni atoms be achieved, but also the difference Fourier map improved from $\Delta\rho_{max/min}$ = 5.57/−5.78 to $\Delta\rho_{max/min}$ = 1.94/−2.41 and the residual factors dropped for R_{obs}(all) from 0.0422 to 0.0379 and for wR_{obs}(all) from 0.0558 to 0.0481.

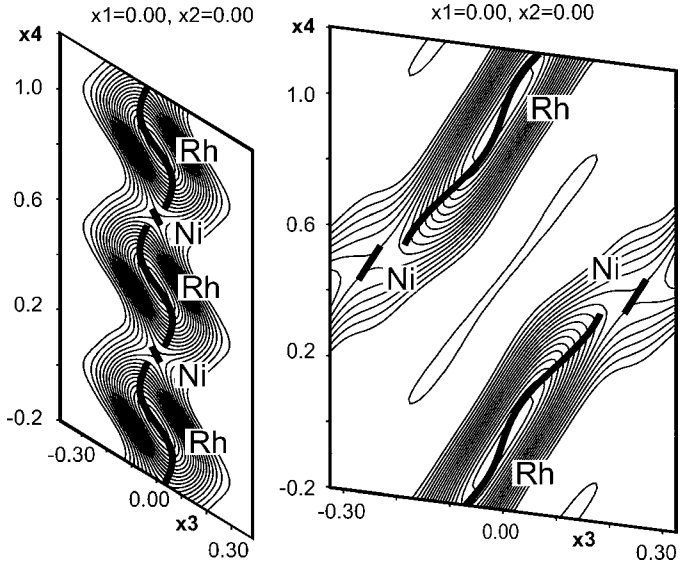

Figure 2
Fourier map in the x_3–x_4 plane (*modulated composite* on the left, *modulated-layer structure* on the right) for Rh and Ni, showing the character of the atomic domains (heavy solid lines) along x_4. The increment of the contour lines is 20 e Å^{-3}.

All final refined parameters are given in the supplementary material.

3.3. Modulated-layer structure

The structure was interpreted as a stacking of two different types of layer (Elcoro *et al.*, 2003). In this approach subsystem 2 with the Ba cations was used as a reference. For this model, the superspace group $X\bar{3}c1(00\gamma)000$ was applied (Elcoro *et al.*, 2003), where X stands for the lattice translations (2/3, 1/3, 0, 2/3) and (1/3, 2/3, 0, 1/3). A detailed explanation on how to derive this space group from $R\bar{3}m(00\gamma)0s$ is given in Elcoro *et al.* (2003). The general stoichiometric formula with respect to the new cell is $AA'_yB_{1-2y}O_{3(1-y)}$. To simplify the notation, the composition-related y parameter was introduced by Elcoro *et al.* (2003) with $y = x/(1 + x) = n/[3(m + n)]$. In this notation the substitution of three O atoms by one Ni atom is stressed (as it is implied by the layer model).

The (idealized) relation between the amplitudes of the sawtooth functions were derived by assuming their parallelism. The structural parameters are given in the supplementary material as a function of the stoichiometric parameter y. Analogous to the *modulated composite*, the Ni, Rh and O atoms are described by sawtooth functions and the atoms Ba1 and Ba2 by crenel functions. In this description, the starting reference model situates the Ba1 atoms at the z level of the centre of the trigonal prisms in a neighbouring $[Ni,Rh]O_3$ column and the Ba2 atoms at the z level of the O_3 triangles. The refinement of the structure in (3 + 1)-dimensional superspace was performed with the program *JANA*2000 (Petricek *et al.*, 2000) in cell setting 2. The final residual values for refining 53 parameters are $R_{obs} = 0.0382$ and $wR_{obs} = 0.0504$ for the observed reflections. More details on the refinement are given in Table 3.

The atomic domains are described with orthogonalized functions. In the first step of refinement, only sawtooth functions for Ni, Rh and O (Elcoro *et al.*, 2003) and crenel functions for Ba1 and Ba2 are applied and successively additional waves are implemented for Rh, O and Ba2, after refining the amplitudes of the sawtooth functions and fixing them to the refined values (see §3.2, describing the refinement of the modulated composite). In the final model, the atomic domains of the Rh and O atoms are described with sawtooth functions and additional two waves for the displacive modulation, and two waves for the modulation of the anisotropic ADPs, the Ba2 atom with a crenel function and one additional wave for the displacive modulation. The modulations of the Ni and Ba1 atoms are described only with the sawtooth function and the crenel function, respectively. The Fourier maps with the atomic domains are given in Figs. 2–4.

The ADPs of the Ni atoms were not positive definite within an harmonic description. After considering the nonharmonic behaviour and introducing Gram–Charlier fourth-order tensor coefficients into the refinement, the ADPs of the Ni

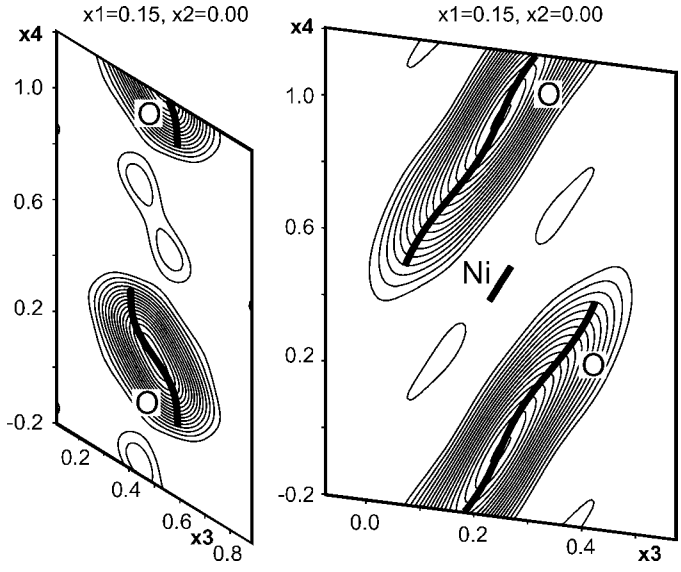

Figure 3
Fourier map in the x_3–x_4 plane (*modulated composite* on the left, *modulated-layer structure* on the right) for O, showing the character of the atomic domains (heavy solid lines) along x_4. The increment of the contour lines is 2 e Å^{-3}. For the *modulated-layer structure* the Ni atom is drawn to demonstrate the substitution of an O_3 triangle by one Ni atom in the $[A_3A'O_6]$ layers.

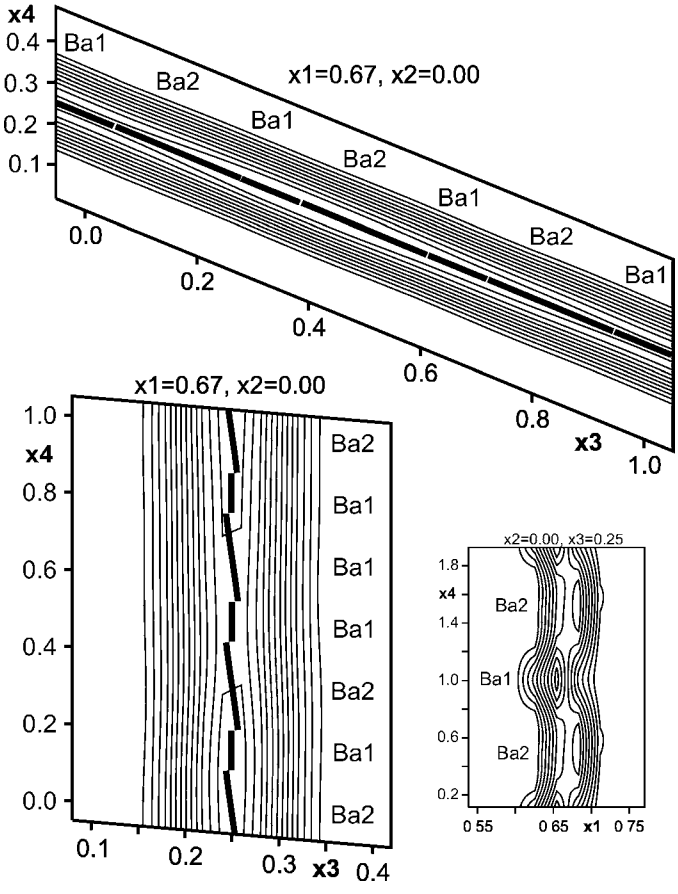

Figure 4
Fourier map in the x_3–x_4 plane for Ba in the modulated composite on the top and in the modulated-layer structure on the left bottom. The atomic domains are drawn as heavy solid lines. The increment of the contour lines is 15 e Å^{-3}. On the right bottom the electron density in the x_1–x_4 plane for Ba in the modulated composite is shown to justify and visualize the discontinuity and the existence of crenels in the Ba modulation.

Table 4
Selected interatomic distances in Å.

The symmetry codes for the O—O distances refer to the respective cell settings in the two structural models.

		Modulated composite	*Modulated-layer structure*
Rh—Rh	Average	2.548 (11)	2.545 (5)
	Min–Max	2.466 (2)–2.652 (14)	2.422 (3)–2.629 (5)
Rh—Ni	Average	2.703 (10)	2.715 (5)
	Min–Max	2.633 (9)–2.769 (11)	2.706 (5)–2.735 (3)
O—Rh	Average	1.99 (3)	1.993 (14)
	Min–Max	1.71 (2)–2.07 (4)	1.768 (14)–2.077 (13)
O—Ni	Average	2.05 (2)	2.106 (13)
	Min–Max	1.98 (2)–2.12 (3)	2.093 (12)–2.131 (13)
O—O	Average	2.64 (6)[i]	2.65 (2)[ii]
	Min–Max	2.20 (4)–2.77 (6)	2.36 (2)–2.77 (2)
O—O	Average	2.96 (3)[iii]	2.951 (13)[iv]
	Min–Max	2.87 (2)–3.00 (3)	2.834 (14)–3.010 (14)
O—O	Average	3.07 (2)[v]	3.139 (15)[i]
	Min–Max	3.065 (19)–3.07 (2)	3.131 (16)–3.153 (13)

Symmetry codes: (i) $-y, x-y, z$; (ii) $-x+y, -x, z$; (iii) $y, -x+y, -z$; (iv) $y, -x+y, 1-z$; (v) $x, y, 1+z$.

atoms became positive. The final refined parameters are given in the supplementary material.

4. Discussion

$Ba_{1+x}Ni_xRh_{1-x}O_3$ is a new member in the family of trigonal compounds of the general formula $A_{1+x}A'_xB_{1-x}O_3$. Using this compound as an example it has been shown that the structure can be described as an intergrowth of $(Ni,Rh)O_3$ columns and (Ba) chains (*modulated composite*) or as a stacking of $[Ba_3O_9]$ and $[Ba_3NiO_6]$ layers with Rh atoms in the octahedral interstices (*modulated-layer structure*). For both models with the same number of refined structural parameters, the statistical parameters of the refinement attained similar values. The *modulated composite* refinement gives slightly better residual parameters, but its set of reflections is slightly smaller, whereas the *modulated-layer structure* refinement gives a somewhat more flat difference-Fourier map (Table 3).

The sets of crenels or atomic domains introduced in these two alternative descriptions define a different reference idealized structure with respect to which actual experimental structure is obtained by means of additional displacive modulations. In this basic reference of the *composite* description the height of the trigonal prisms along the z axis is equal to that of the octahedra, whereas the adjacent Ba atoms distribute equidistantly along z with a period incommensurate with this height. Necessarily, O and Ba atoms then have different z-coordinates. On the other hand, in the reference of the *modulated-layer* description, the trigonal prisms have double height relative to the octahedra, and Ba and O have equal z values, as they correspond to the idealized layers.

In the description as *modulated composite* the approximate one-dimensional character of the structure is highlighted, stressing the intra-subsystem interactions (*e.g.* the Ni—O and Rh—O bonds) which are in general stronger than the inter-subsystem interactions. Considering two subsystems and choosing the one with the smaller cell as a reference, this model maximizes the number of main reflections and minimizes the number of satellite reflections. In the refinement as a *modulated-layer structure* the close relation to the 2*H* hexagonal perovskite is implemented. In this description the structure is understood in a first approximation as a hexagonal close packing of $[A_3O_9]$ and $[A_3A'O_6]$ layers. Some stiffness of the layers is implied. Under this approach, the various composition-dependent layer stacking sequences underlying this type of structure are predicted and used as the starting point for the refinement (Elcoro *et al.*, 2003).

The inclusion of sawtooths as a first step for the displacive modulations of the O atoms introduces in both descriptions a first global deviation of the ratio of the heights of prisms and octahedra from their respective ideal values. The heights are equal for all octahedra and all prisms, but their relative values were no longer fixed. The superposition of additional waves on the sawtooth functions consequently means that all prisms and octahedra are no longer equal, but have their own specific slight deformation. In the *modulated-layer* description (this implies that the $[A_3O_9]$ and $[A_3A'O_6]$ layers deform according to the modulations, also becoming inequivalent. Through the refinement of these atomic displacive modulations, both descriptions should in principle arrive at the same model for

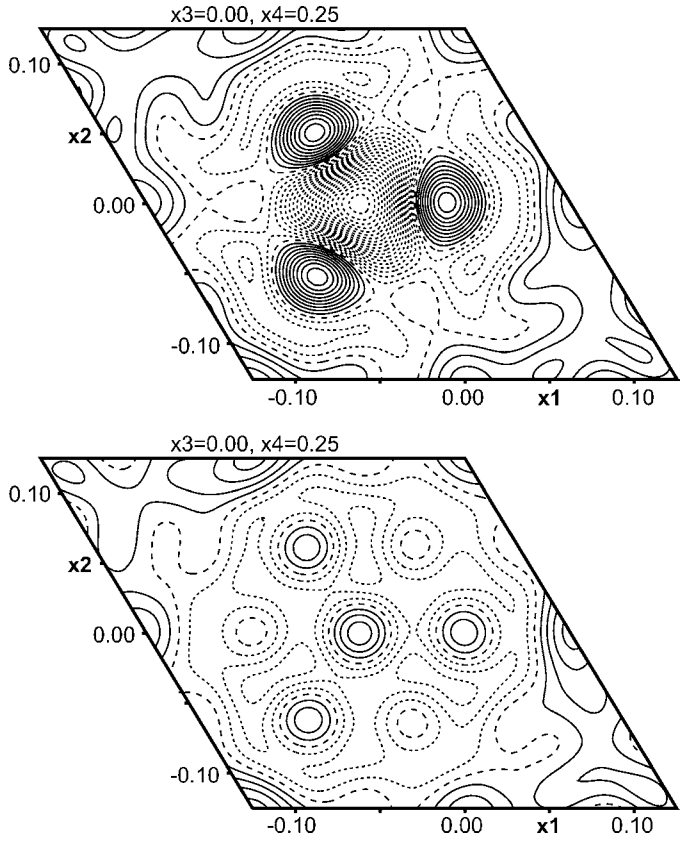

Figure 5
Difference Fourier map in the x_1–x_2 plane (*modulated composite*) showing the nonharmonic character of the Ni atom, above the result of the refinement with harmonic ADPs ($\Delta\rho$ = 1.95/−3.93 e Å^{-3}), below with Gram–Charlier nonharmonic terms of fourth order ($\Delta\rho$ = 0.89/−0.72 e Å^{-3}). The increment of the contour lines is in both cases 0.2 e Å^{-3}. The $\Delta\rho$ given here refer to the sections shown and not to the complete unit cell.

the real three-dimensional structure. It is only the reference with respect to which these modulations are defined that varies from one description to the other. The refinements indeed reach similar quality values, as discussed above, and the resulting three-dimensional structural models are indeed very similar. Nevertheless, the two models introduce a perturbative approach with respect to different reference configurations and the refined displacive modulations are constrained by the cut-off of the respective series expansions. This necessarily introduces some bias when using one or the other model. This becomes apparent when the interatomic distances of the models are compared.

In Figs. 6 and 7 the Rh—Ni, Rh—Rh, O—Ni, O—Rh and O—O distances are presented as functions of *t*. The internal coordinate *t* has a different meaning in the two descriptions, so the curves are not directly comparable. It is the resulting distance distributions that may be compared. The main features of these distributions are listed in Table 4. Both distance sets essentially agree in the basic features. The Rh—Ni and O—Ni distances are significantly larger than the Rh—Rh and O—Rh distances, respectively: the average value for O—Ni is around 2.1 Å, while the average value for O—Rh is around 2.0 Å. The Rh—Rh distances are around 2.55 Å, whereas the Rh—Ni distances (octahedron-prism) are larger, as expected, with an average value of 2.7 Å. From the shape of the curves of Rh—Rh distances it also becomes clear that the end Rh atoms (those closer to the prisms) are displaced towards the prisms, which is manifested in the shorter O—Rh distances. This is in agreement with the observations in related compounds, *e.g.* $Ba_{1+x}RhO_3$ (Stitzer *et al.*, 2004), where the shortest metal–metal distance corresponds to the middle of the octahedra sequence (see also Fig. 1). The heights of the trigonal prisms D_p are clearly larger than those of the octahedra D_o. In the ideal *composite* model, both have to be the same, $D_p = D_o$; in the ideal *layer* model the relation should be $D_p = 2D_o$. Taking the Rh—Rh distances as the heights of the octahedra, they are *ca* $D_o \simeq 2.55$ Å and the results are the same in the two models to within standard errors. The average height of the trigonal prisms is defined by the corresponding O—O distance along the *z* axis. This average distance is the only one that significantly differs between the two models. $D_p \simeq 3.07 \pm 0.02$ Å and $D_p \simeq 3.14 \pm 0.02$ Å, for the *modulated composite* and the *modulated-layer structure*, respectively. Therefore, the ratio between the prism and the octahedral average heights is *ca* $D_p = 1.20D_o$ in the description as *modulated composite* and $D_p = 1.24D_o$ in the description as a *modulated-layer structure*. Each refined model seems then biased in this respect by the alternative starting reference value for the prism height.

Concerning the range of the distance distributions, Figs. 6 and 7 show some clear differences between the two models. For the Rh—Ni distances, the distance range between the minimum and maximum value is larger in the *modulated composite* than in the *modulated-layer structure*, which is also reflected in the O—Ni distances. However, the *modulated composite* gives a more homogenous result for the O—O distances, as seen in Fig. 7. These differences are, however, not very significant. One should take into account that these

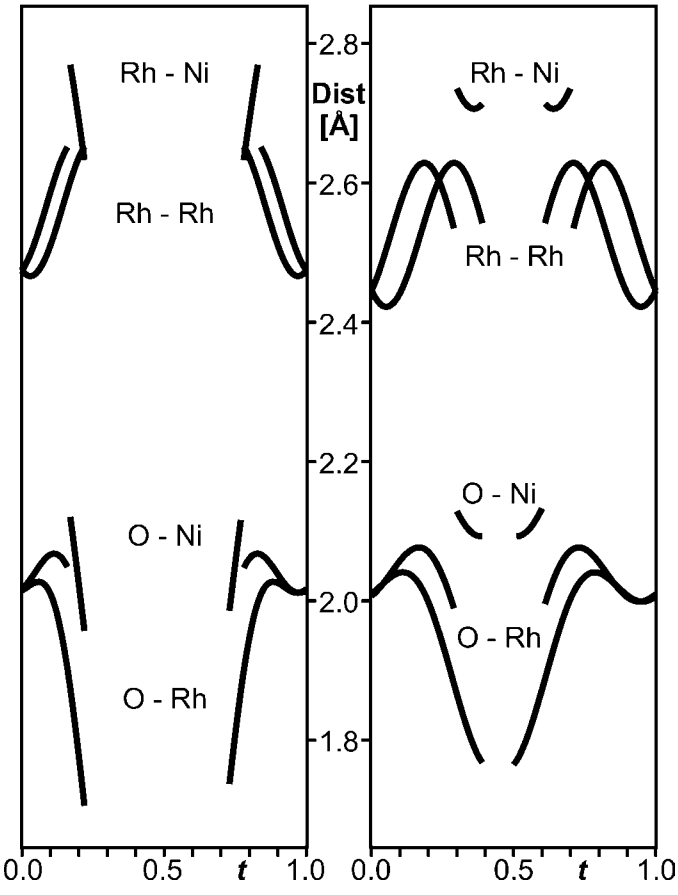

Figure 6
Interatomic distances in Å as a function of the internal *t* coordinate in the *modulated composite* on the left and in the *modulated-layer structure* on the right.

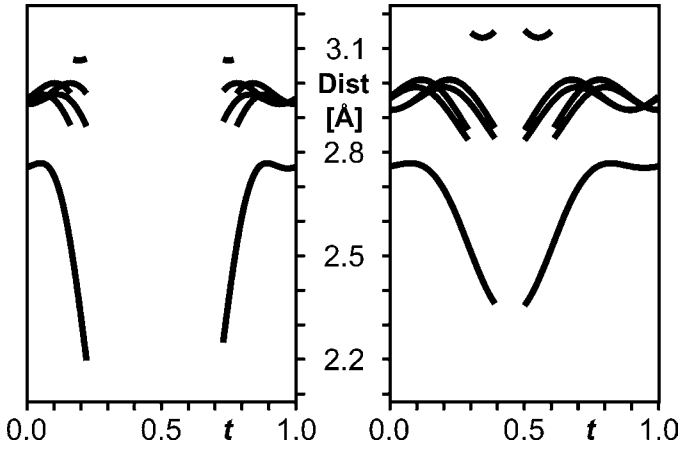

Figure 7
Interatomic O—O distances in Å as a function of the internal *t* coordinate in the *modulated composite* on the left and in the *modulated-layer structure* on the right. The distances around 3.1 Å correspond to the height of the trigonal prisms, those around 3.0 Å to O atoms of consecutive triangles along the *z* direction and those around 2.5 Å to O atoms in the same triangle with similar *z* coordinates.

changes in the range of the distances are in general due to rather steep parts of the distance curves along t, and this means that the weights of these sets of distance values in the whole distributions are minimal. This reflects a general problem of the description of incommensurate or long-period structures as modulated structures. Through the modulations in fact an infinite or very large number of inequivalent atoms is described and changes in the modulations that are limited to a minimal proportion of these atoms will cause a negligible variation in the fit quality of the model.

5. Conclusions

The superspace approach is a powerful tool for the description of these $A_{1+x}A'_xB_{1-x}O_3$ compounds. The stoichiometry can be obtained from the diffraction pattern by a simple refinement of the lattice parameters before starting the structure solution and refinement. A small variation in stoichiometry causes a dramatic change in the classical three-dimensional superstructure model, but it results in only a slight variation in the (3 + 1)-dimensional superspace models.

The descriptions *modulated composite* and *modulated-layer structure* use two alternative and idealized models for these compounds as the starting configuration for the refinement. Although some slight differences can be observed between the resulting three-dimensional structures for the two refined models, a definite choice between them is not possible. Both models can describe the observations well with a similar number of parameters.

This work has been supported by the DFG (Deutsche Forschungsgemeinschaft) and the UPV/EHU (Universidad del País Vasco). We gratefully thank Luis Elcoro for very valuable comments and discussion.

References

Battle, P. D., Blake, G. R., Darriet, J., Gore, J. G. & Weill, F. (1997). *J. Mater. Chem.* **7**, 1559–1564.
Battle, P. D., Blake, G. R., Sloan, J. & Vente, J. F. (1998). *J. Solid State Chem.* **136**, 103–114.
Blake, G. R., Sloan, J., Vente, J. F. & Battle, P. D. (1998). *Chem. Mater.* **10**, 3536–3547.
Darriet, J. & Subramanian, M. A. (1995). *J. Mater. Chem.* **5**, 543–552.
El Abed, A., Elqebbaj, S. E., Zakhour, M., Champeaux, M., Perez-Mato, J. M. & Darriet, J. (2001). *J. Solid State Chem.* **161**, 300–306.
Elcoro, L., Perez-Mato, J. M., Darriet, J. & El Abed, A. (2003). *Acta Cryst.* B**59**, 217–233.
Evain, M., Boucher, F., Gourdon, O., Petricek, V., Dusek, M. & Bezdicka, P. (1998). *Chem. Mater.* **10**, 3068–3076.
Gourdon, O., Petricek, V., Dusek, M., Bezdicka, P., Durovic, S., Gyepesova, D. & Evain, M. (1999). *Acta Cryst.* B**55**, 841–848.
Henley, W. H., Claridge, J. B., Smallwood, P. L. & zur Loye, H.-C. (1999). *J. Cryst. Growth*, **204**, 122–127.
Janner, A. & Janssen, T. (1980*a*). *Acta Cryst.* A**36**, 399–407.
Janner, A. & Janssen, T. (1980*b*). *Acta Cryst.* A**36**, 408–415.
Janssen, T., Janner, A., Looijenga-Vos, A. & de Wolff, P. M. (1992). *International Tables for Crystallography*, Vol. C, edited by A. J. C. Wilson, pp. 797–835. Dordrecht: Kluwer Academic Publishers.
Kuhs, W. F. (1992). *Acta Cryst.* A**48**, 80–98.
Neville, E. H. (1950). *Royal Society Mathematical Tables*, Vol. 1, *The Farey Series of Order 1025*. Cambridge: Royal Society/Cambridge University Press.
Oxford Diffraction (2003). *CrysAlis Software Package*, Version 170. Oxford Diffraction *sp.*Zo.o, Wroclaw, Poland.
Perez-Mato, J. M., Madariaga, G., Zuñiga, F. J. & Garcia Arribas, A. (1987). *Acta Cryst.* A**43**, 216–226.
Perez-Mato, J. M., Zakhour-Nakhl, M., Weill, F. & Darriet, J. (1999). *J. Mater. Chem.* **9**, 2795–2808.
Petricek, V., Dusek, M. & Palatinus, L. (2000). *JANA*2000. The Crystallographic Computing System. Institute of Physics, Praha, Czech Republic.
Petricek, V., Gao, Y., Lee, P. & Coppens, P. (1990). *Phys. Rev.* **42**, 387–392.
Petříček, V., van der Lee, A. & Evain, M. (1995). *Acta Cryst.* A**51**, 529–535.
Schönleber, A., Meyer, M. & Chapuis, G. (2001). *J. Appl. Cryst.* **34**, 777–779.
Smaalen, S. van (1995). *Crystallogr. Rev.* **4**, 79–202.
Stitzer, K. E., El Abed, A., Darriet, J. & zur Loye, H.-C. (2004). *J. Am. Chem. Soc.* **126**, 856–864.
Ukei, K., Yamamoto, A., Watanabe, Y., Shishido, T. & Fukuda, T. (1993). *Acta Cryst.* B**49**, 67–72.
Wolff, P. M. de (1974). *Acta Cryst.* A**30**, 777–785.
Zakhour-Nakhl, M., Claridge, J. B., Darriet, J., Weill, F., zur Loye, H.-C. & Perez-Mato, J. M. (2000). *J. Am. Chem. Soc.* **122**, 1618–1623.
Zakhour-Nakhl, M., Darriet, J., Claridge, J. B., zur Loye, H.-C. & Perez-Mato, J. M. (2000). *Int. J. Inorg. Mater.* **2**, 503–512.
Zakhour-Nakhl, M., Weill, F., Darriet, J. & Perez-Mato, J. M. (2000). *Int. J. Inorg. Mater.* **2**, 71–79.